REVIEW

Check for updates

Journal of
Sensor Science and Technology

The Korean Sensors Society

Flash-Thermal Shock Synthesis of Nanomaterials and Catalysts for Chemical Sensing

Suk-Jeong Kwon[1], Sungwoo Eo[1], Ji-Hwan Eum[1], and Dong-Ha Kim[1,+]

[1]*Department of Materials Science and Chemical Engineering, Hanyang University, Ansan 15588, Republic of Korea*

Cite This: *J. Sens. Sci. Technol. Vol. 35, No. 4 (2026) 330-341*

https://doi.org/10.46670/JSST.2026.35.4.330

ABSTRACT: Flash-thermal shock (FTS) synthesis is a nonequilibrium processing strategy for rapidly tailoring nanomaterials and catalysts through millisecond-scale high-temperature pulses. By localizing photothermal energy within a short time window, FTS can induce precursor decomposition, reduction, defect generation, phase transformation, and catalyst immobilization while suppressing grain growth, sintering, and thermal degradation. These features are particularly useful for chemical gas sensors, where surface defects, interfacial charge transfer, catalytic activity, and structural stability strongly affect sensing performance. This review focuses on intense pulsed light (IPL)-driven FTS as a scalable, non-contact photothermal route for designing sensing materials. We first discuss representative rapid annealing techniques, photothermal mechanisms, and material-selection criteria for efficient FTS. We then summarize FTS-enabled engineering of carbon materials, metal oxides, transition metal dichalcogenides, and carbides, with emphasis on defect control, phase reconstruction, heterointerface formation, and sensing-relevant transport modulation. Catalyst design strategies involving high-entropy alloys, single-atom catalysts, and ex-solution catalysts are further discussed in relation to gas activation and selectivity control. Finally, we outline current challenges and future opportunities for advancing FTS-derived materials for next-generation chemical sensing.

KEYWORDS: *Intense pulsed light, Flash-thermal shock, Photothermal effect, Catalysts, Chemical gas sensors*

1. INTRODUCTION

The design of nanomaterials and catalysts for chemical sensing requires synthetic routes that can precisely control surface chemistry, defect structures, phase composition, and catalyst–support interactions [1,2]. These features strongly influence gas adsorption, charge transfer, catalytic dissociation, and ultimately sensing performance, yet they are often difficult to optimize through conventional furnace-based synthetic routes [3,4]. Because equilibrium heating typically involves prolonged thermal exposure, it can promote grain coarsening, interdiffusion, phase over-stabilization, and unwanted degradation of nanostructures. As a result, there is growing interest in nonequilibrium thermal approaches that can drive rapid structural and chemical transformations while preserving or enhancing nanoscale functionality [5-7]. In this context, flash-thermal shock (FTS) has gained increasing attention as a distinctive photothermal strategy for the synthesis of sensing materials with tunable defects, metastable phases, engineered interfaces, and catalytically active surface sites [8,9].

In this review, we examine FTS as a materials engineering platform for the synthesis and functionalization of nanomaterials and catalysts relevant to chemical sensing. Among the various advanced annealing techniques, FTS offers distinctive advantages for rapid and non-equilibrium nanomaterial engineering, and we therefore examine this approach in depth. While other rapid thermal processing strategies are briefly discussed for comparison, this review primarily focuses on IPL-driven FTS and its applications in sensing-material engineering (Table 1). We then discuss its fundamental photothermal mechanisms and the key criteria that govern material selection. We next summarize how FTS enables diverse nanoengineering pathways, including surface defect generation and reconstruction, heterostructure and interfacial phase engineering, and catalyst design across high-

[+]Corresponding author: dongha0507@hanyang.ac.kr
Received : Jun. 5, 2026, Revised : Jun. 10, 2026, Accepted : Jun. 24, 2026

Table 1. Summary and evaluation of nonequilibrium synthesis methods.

Method	IPL-driven FTS	Microwave heating	Laser annealing	Joule-heating
Energy source	Xenon flash lamp	Microwave radiation	Coherent laser beam	Electrical current
Heating mechanism	Photothermal conversion	Dielectric heating	Photothermal conversion	Resistive heating
Scalability	High	Medium	Low	Medium
Applicable materials	Broad	Moderate	Broad	Very narrow
Key limitations	Film thickness and atmosphere control	Limited by microwave absorptivity	Limited large-area uniform processing	Limited by material conductivity

entropy, single-atom, and ex-solution systems. Through these examples, we highlight how millisecond-scale photothermal processing expands the accessible design space of sensing materials beyond that of conventional thermal treatments. Finally, we discuss the remaining challenges and future directions for translating FTS into a more general and reliable platform for next-generation chemical sensing materials.

2. PRINCIPLES OF PHOTOTHERMAL SYNTHESIS

2.1 Advanced annealing techniques

Advanced annealing techniques can be systematically categorized according to their energy source and heating mechanism. Light-based approaches, including laser irradiation and xenon-lamp intense pulsed light (IPL), induce rapid heating through photothermal light–material interctions [10,11]; Joule heating relies on resistive heat generation under applied current [12], and microwave or arc heating uses electromagnetic or plasma-based energy delivery [13-15]. While each method provides access to ultrafast thermal processing, their applicability differs in terms of spatial uniformity, scalability, controllability, and materials compatibility. Laser annealing offers excellent spatial precision but limited large-area processability, whereas Joule heating is highly efficient but generally restricted to conductive systems [16-21]. Microwave and arc heating can reach rapid or ultrahigh-temperature regimes, but often face challenges in heating uniformity and process stability [22-27]. By contrast, IPL-driven FTS uniquely combines broadband absorption, non-contact large-area irradiation, ultrafast heating and quenching, and ambient-process compatibility, making it especially attractive for the synthesis of non-equilibrium

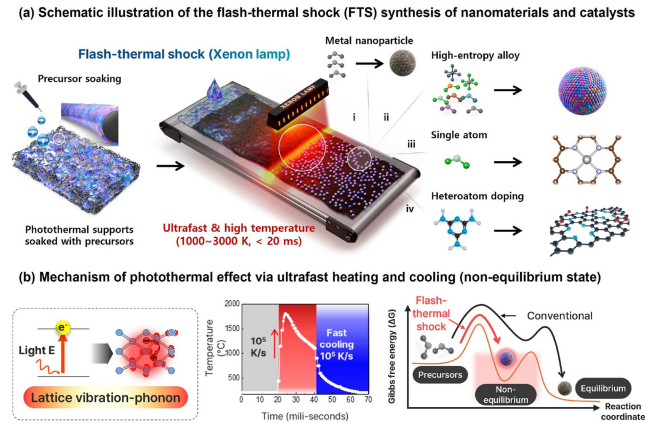

Fig. 1. Principles of the flash-thermal shock (FTS) method. (a) Schematic illustration of the FTS-driven synthesis of nanomaterials and catalysts. Adapted from Ref. [31]. (b) Schematic illustration of the photothermal mechanism of FTS.

nanomaterials (Fig. 1(a)) [28-33]. As a result, IPL-driven FTS has emerged as a versatile kinetic-control platform for accessing advanced metastable structures and functional nanointerfaces beyond the reach of conventional annealing.

2.2 Flash-thermal shock mechanisms

FTS is driven by the rapid conversion of broadband light into highly localized thermal energy. Under xenon-flash irradiation, photons are absorbed by the light-responsive host material and converted into heat via non-radiative relaxation processes (Fig. 1(b)) [34]. Because this conversion occurs within a millisecond pulse, the irradiated region can reach extremely high temperatures in a very short time, while heat diffusion into the bulk remains limited. This creates a transient nonequilibrium thermal state in which the surface is strongly

heated, but the underlying substrate remains relatively cool and can function as a heat sink. In this way, FTS enables spatially confined, surface-selective thermal processing that is fundamentally different from conventional furnace annealing.

This unique thermal environment directly governs the reaction pathway during materials synthesis. The intense but short-lived heating rapidly activates nearby precursor species, triggering decomposition, reduction, diffusion, and nucleation within an exceptionally narrow time window. However, because the subsequent quenching is also extremely fast, long-range atomic diffusion, grain growth, and phase separation are strongly suppressed before the system can fully relax toward equilibrium. As a result, FTS favors kinetic trapping of non-equilibrium structures, enabling the formation of metastable phases, defect-rich surfaces, single atoms, ultrafine nanoparticles, and heterostructured interfaces that are difficult to obtain through slow, equilibrium-based annealing [9,31,32,35,36].

2.3 Flash-thermal shock material design

The feasibility and efficiency of FTS should be considered not simply in terms of whether a material absorbs light, but more systematically from the perspectives of optical absorption, photothermal conversion, and thermal dissipation. Materials with strong broadband absorption and efficient non-radiative relaxation are the most favorable photothermal hosts. Representative examples include carbonaceous materials such as carbon nanotubes, carbon nanofibers, graphene/rGO, and carbon black, as well as dark or nonstoichiometric oxides such as Fe_3O_4, Co_3O_4, CuO, WO_{3-x}, and black TiO_2. In selecting materials, both the magnitude of the band gap and the nature of the electronic transition are important, as they govern not only photon absorption but also the efficiency with which the absorbed energy is converted into lattice heat. In general, indirect-gap materials or defect-rich systems can promote phonon-assisted non-radiative relaxation more effectively than direct-gap, weakly absorbing counterparts, although the overall photothermal efficiency also depends on defect states, carrier lifetime, and electron–phonon coupling. Thermal transport must also be considered because FTS performance is strongly influenced by how quickly the generated heat is dissipated. Reducing grain size, increasing grain-boundary density, or introducing thermally insulating interlayers beneath the active layer can suppress heat loss, slow cooling, and effectively extend the annealing window. Even when the target material itself has a wide band gap and poor photothermal response, FTS can still be realized by coupling it with a highly absorbing carbon membrane or carbon scaffold, so that the carbon component serves as a photothermal heater and transfers heat to the wide-band-gap phase through interfacial conduction and local convection. Therefore, rational materials design for FTS requires simultaneous consideration of optical absorption, electronic structure, non-radiative energy dissipation, and heat-flow management, rather than band gap alone.

3. FLASH-THERMAL SHOCK FOR PHASE ENGINEERING

3.1 Surface defects engineering and reconstructions

The FTS process delivers an ultrafast, high-temperature shock to the surface of nanomaterials, enabling precise modulation of surface defect states and, in some cases, surface reconstruction. One representative example is the photothermal reduction of graphene oxide (GO) to reduced graphene oxide (rGO) [37,38]. Even brief irradiation with an intense light source can partially reduce GO, accompanied by a visible color change from brown to black, reflecting the restoration of conductive carbon networks.

Choi et al. employed FTS to optically reduce GO and fabricate an rGO-based NO_2 gas sensor on a wearable platform incorporating an Ag nanowire-embedded colorless polyimide (cPI) film [39]. The localized and short-duration FTS treatment minimized thermal damage to the cPI substrate while simultaneously welding the Ag nanowires to form an electrically connected conductive/heating layer. At the same time, the formation of rGO provided percolative charge-transport pathways for chemiresistive sensing. Temperature-controlled operation using the Ag NW-cPI heater accelerated NO_2 sensing kinetics, enabling faster adsorption and desorption and supporting wearable patch-type sensor operation.

In addition to simple GO reduction, simultaneous heteroatom doping can be achieved by incorporating boric acid as a boron source (Fig. 2(a)) [40]. When an FTS process is applied to a GO/boric acid mixed film at a temperature exceeding the decomposition point of boric acid, boron is successfully incorporated into the rGO framework, yielding p-type B-doped rGO. This material exhibited a 5.4-fold higher NO_2 sensing response at 5 ppm than pristine rGO. Follow-up work further showed that mixing GO with melamine as a nitrogen source enabled the formation of n-type N-doped rGO through the same FTS strategy. These results highlight that both p-type and n-type graphene can be readily synthesized by FTS through the simple selection of suitable doping sources.

More recently, Eum et al. reported the synthesis of rGO by FTS, followed by the growth of conductive metal-organic frameworks (cMOFs) on the rGO surface through a layer-by-layer method to construct rGO@cMOF composites (Fig. 2(b)) [41]. Because this growth relies on surface functional groups,

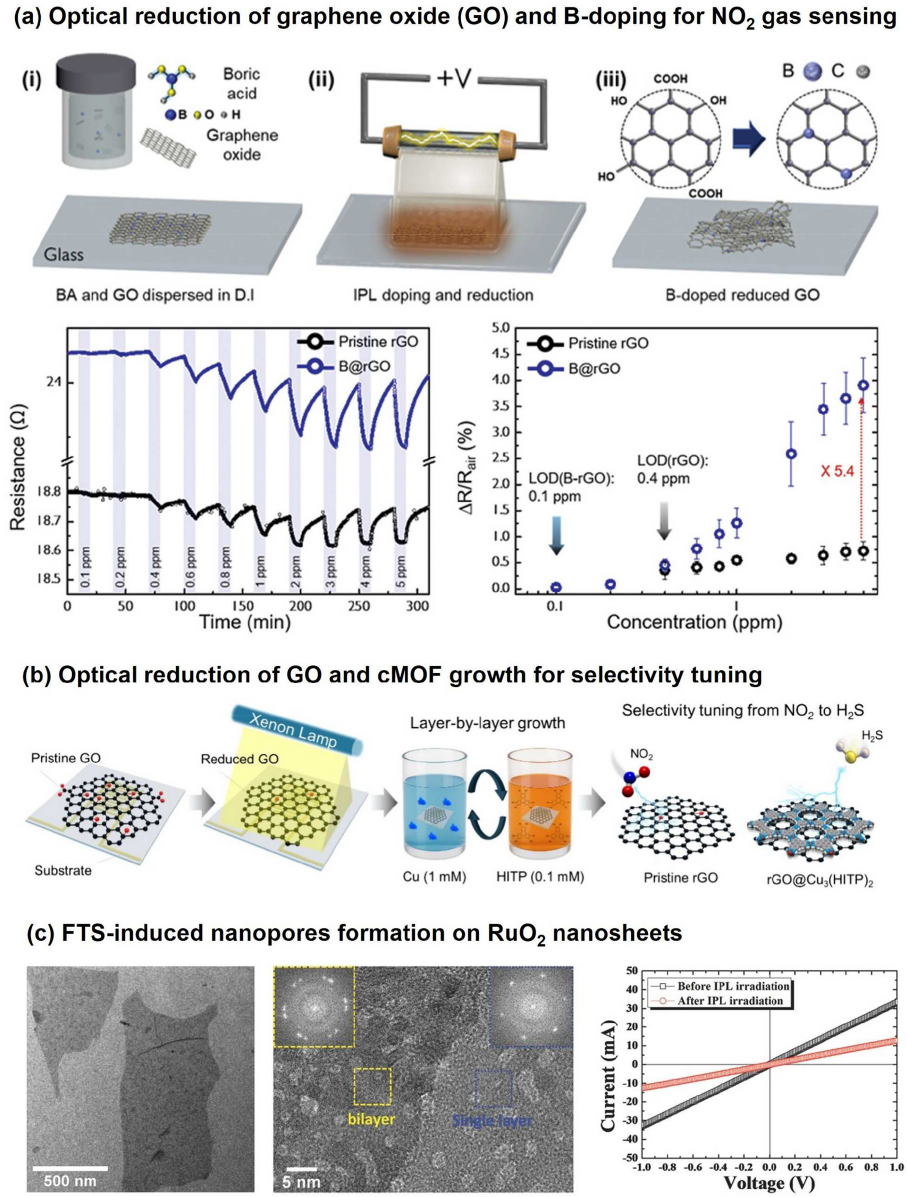

Fig. 2. FTS for surface defects engineering and reconstructions. (a) Synthesis of boron-doped rGO for enhanced gas-sensing performance. Adapted from Ref. [40]. (b) Growth of conducting metal–organic frameworks on optically reduced GO. Adapted from Ref. [41]. (c) Schematic illustration of nanopore formation in 2D RuO_2 via FTS. Adapted from Ref. [42].

the density of residual oxygen-containing groups on rGO, such as hydroxyl and carboxyl species, plays a critical role in determining the nucleation behavior of cMOFs. By optimizing the FTS reduction conditions and subsequent cMOF growth, the resulting composites exhibited significantly enhanced H_2S sensing while suppressing the intrinsic NO_2 selectivity of pristine rGO, thereby demonstrating effective selectivity tuning through interfacial engineering. In this respect, FTS-driven optical reduction of GO is not only an effective route to improve conductivity, but also a useful strategy for generating chemically tunable surfaces for subsequent hybrid-material construction.

Another important capability of FTS is the generation of surface defects and nanopores in ultrathin two-dimensional nanomaterials. For example, FTS treatment of RuO_2 nanosheets induced the formation of oxygen vacancies, as confirmed by XPS, together with sub-2 nm nanopores on the nanosheet surface (Fig. 2(c)) [42]. These structural features are highly beneficial for gas sensing. For example, defect sites can serve as energetically favorable adsorption centers, while nanopores can shorten diffusion pathways and facilitate rapid gas transport. Accordingly, FTS provides a versatile platform for defect engineering and nanoscale surface reconstruction, both of which are valuable for improving the sensitivity, selectivity, and response kinetics of chemical sensors.

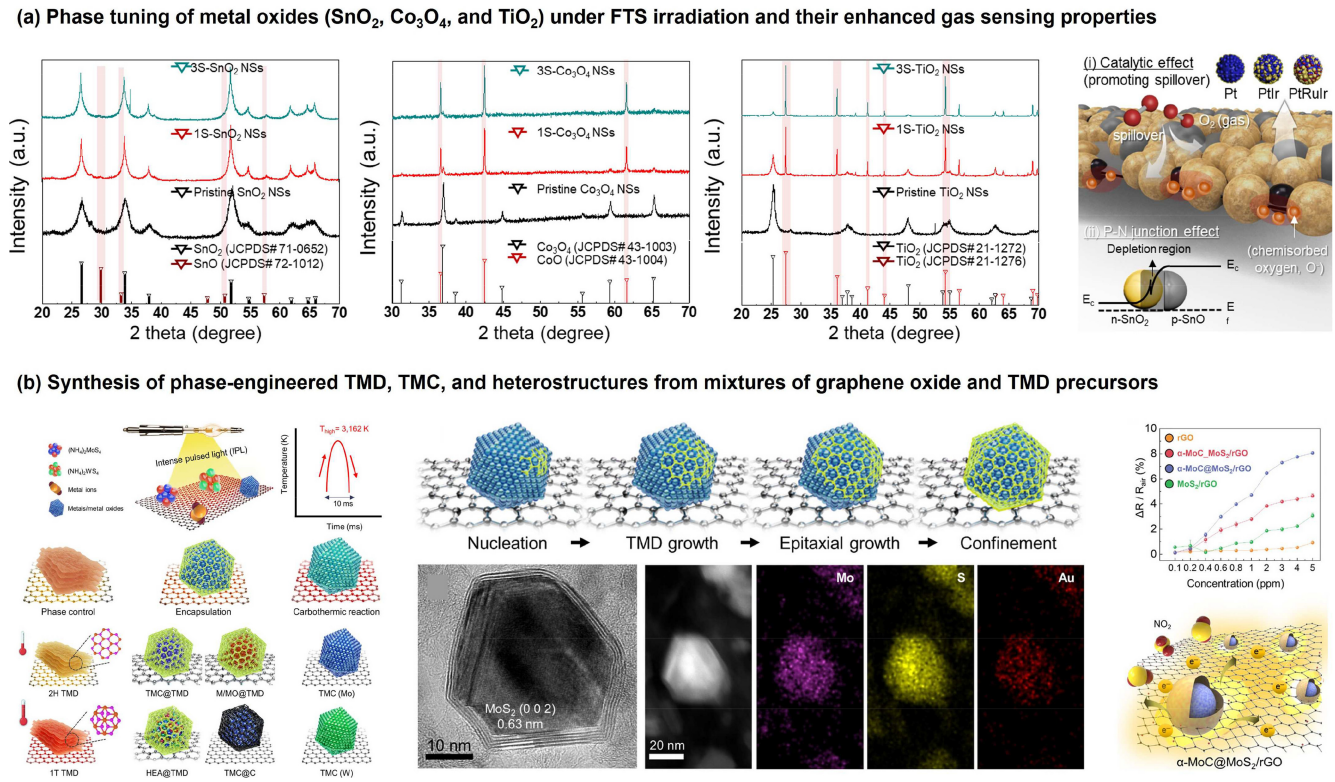

Fig. 3. FTS-driven phase tuning and heterostructure engineering. (a) XRD patterns of SnO_2, Co_3O_4, and TiO_2 before and after FTS treatment with 1 shot (1S) and 3 shots (3S). In the case of SnO_2, partial phase reduction from SnO_2 to SnO forms local n–p heterojunctions, which are beneficial for enhanced gas-sensing performance. Adapted from Ref. [9]. (b) Schematic illustrations of various phase-engineered transition metal dichalcogenides (TMDs) and transition metal carbides (TMCs) synthesized from mixtures of graphene oxide and TMD precursors. When seed materials are additionally introduced, rGO@seed@TMD heterostructures are formed, as illustrated using Au in the schematic. These heterostructures exhibit enhanced NO_2 sensing performance. Adapted from Ref. [33].

3.2 Heterostructure and interfacial phase engineering

FTS is also highly effective for interfacial phase engineering and heterostructure formation in ceramic nanomaterials. Kim et al. showed that FTS treatment of SnO_2 and Co_3O_4 nanosheets induced surface reduction from SnO_2 to SnO and from Co_3O_4 to CoO (Fig. 3(a)) [9]. Importantly, the extent of this phase transition could be precisely tuned by controlling the FTS intensity and the number of pulses, allowing modulation of the heterostructure composition in SnO_2/SnO and Co_3O_4/CoO systems. In particular, because SnO_2 is an n-type semiconductor whereas SnO is p-type, a single FTS process enabled direct formation of n–p SnO_2/SnO heterostructures. In a related example, TiO_2 underwent an anatase-to-rutile phase transition under FTS, highlighting that this millisecond-scale thermal shock can rapidly induce phase transformation while preserving nanoscale morphology.

Beyond metal oxides, FTS can be extended to the synthesis of transition metal carbides (TMCs) and transition metal dichalcogenides (TMDs) through carbon-assisted photothermal processing. For example, GO can serve as an efficient photothermal support, reducing to rGO while simultaneously generating intense localized heat that decomposes precursors and drives phase evolution. Shin et al. demonstrated that GO-based FTS reached tunable peak temperatures of up to 3162 K within 10 ms in air, enabling direct TMD formation at lower temperatures and carbothermic conversion to carbide phases at higher temperatures (Fig. 3(b)) [33]. By controlling the photothermal temperature, phase-engineered MoS_2 was selectively synthesized, including 2H-rich MoS_2 at 1768 K, mixed 1T/2H MoS_2 at 2369 K, and 1T-rich MoS_2 at 2519 K. In addition, α-MoC and α-MoC@MoS_2 nanoparticles were formed on rGO using GO as the carbon source. Similar protocols using different precursors also enabled the synthesis of 1T-WS_2 and tungsten carbide/oxycarbide products. These phase- and interface-engineered nanocomposites exhibited strong performance in gas sensing and electrocatalysis; for instance, α-MoC@MoS_2/rGO showed a 9.2-fold higher NO_2 response at 5 ppm than pristine rGO.

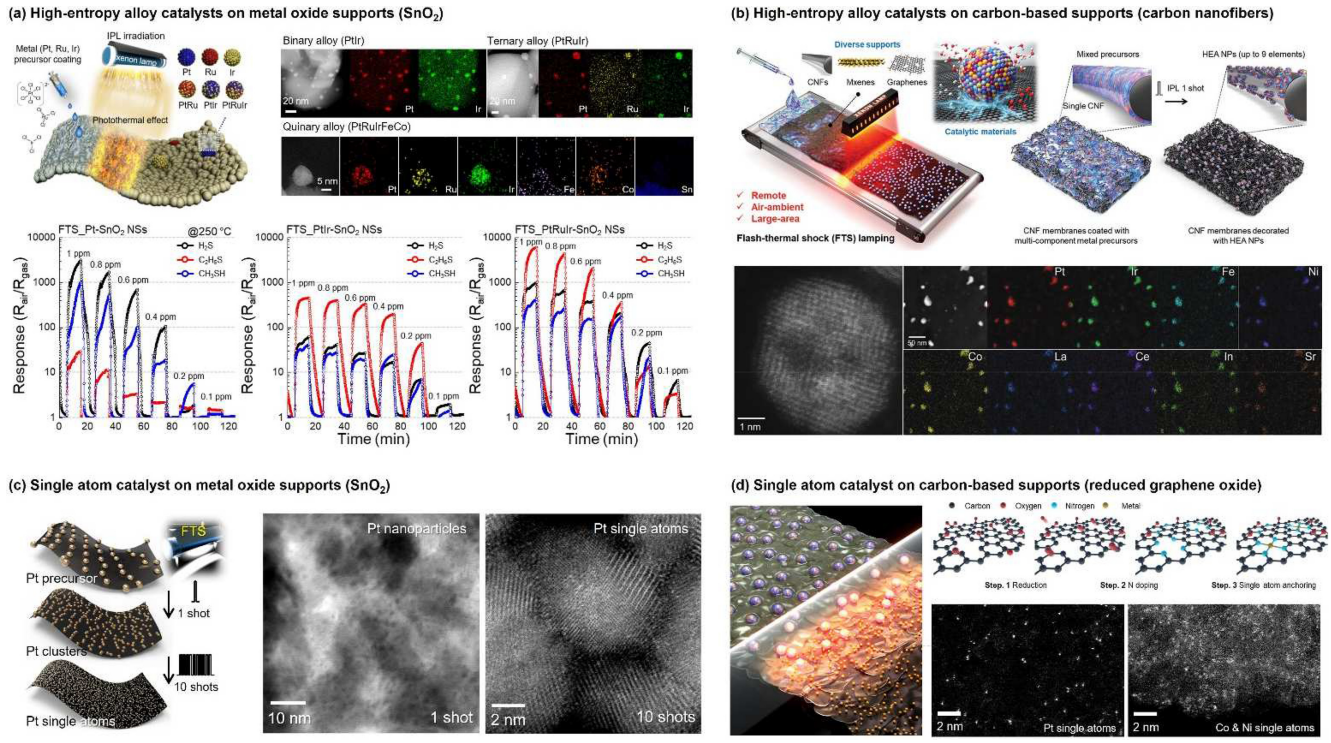

Fig. 4. Schematic illustrations of high-entropy alloy (HEA) and single-atom catalyst (SAC) synthesis using the FTS technique. (a) Synthesis of HEAs on metal oxide supports and their applications in gas sensing toward H_2S, CH_3SH, and C_2H_6S. Adapted from Ref. [9]. (b) Synthesis of HEAs on various carbon-based supports, including an example of PtIrFeNiCoLaCeInSr HEA nanoparticles. Adapted from Ref. [31]. (c) Synthesis of SACs on metal oxide supports using multiple FTS shots; a single shot induces nanoparticle formation, whereas 10 shots lead to SAC formation. Adapted from Ref. [9]. (d) Schematic illustration of SAC formation on N-doped rGO via M–N_4 binding sites, which are advantageous for stabilizing isolated metal atoms. Adapted from Ref. [32].

4. FLASH-THERMAL SHOCK FOR SYNTHESIS OF CATALYSTS

4.1 High-entropy alloy catalysts

High-entropy alloy (HEA) catalysts, which consist of single nanoparticles containing five or more elements, often exhibit unprecedented catalytic properties that are difficult to achieve in single-component systems due to their complex atomic configurations and synergistic multielement effects [43-45]. Therefore, the synthesis of HEAs requires simultaneous promotion of elemental interdiffusion and suppression of phase separation during cooling. In this regard, FTS offers a powerful synthetic platform by providing both thermodynamic and kinetic advantages. Specifically, ultrahigh temperatures (> 2,000 K) enhance multielement mixing by amplifying the configurational entropy contribution, thereby enabling the formation of single-phase solid solutions even among otherwise immiscible elements. Subsequently, ultrafast quenching kinetically traps the mixed state by inhibiting diffusion-driven segregation, preserving the highly distorted atomic configuration. As a result, FTS enables the synthesis of single-phase HEA nanoparticles beyond the limitations of conventional alloying approaches.

Kim et al. demonstrated that FTS enabled the synthesis of HEA nanoparticles on metal oxide-based supports by promoting rapid elemental interdiffusion during ultrafast heating and suppressing phase separation during quenching (Fig. 4(a)) [9]. The synthetic route is straightforward, involving support preparation, mixing with metal precursors in ethanolic solution, drying, and FTS treatment. During this process, the strong photothermal effect of the supports induces rapid precursor decomposition and crystallization, yielding high-density, ultrasmall (< 10 nm) HEA nanoparticles on the support surface. They also showed that sufficiently high processing temperatures are critical for uniform alloy formation, particularly in carbon-supported systems involving carbothermal reactions (Fig. 4(b)) [31]. The applicable substrates are not limited to carbon nanofibers and graphene oxide, but can be expanded to MXenes for HEA formation and functionalization. Moreover, xenon-flash IPL enabled uniform HEA formation over a 6.0 × 6.0 cm^2 carbon nanofiber membrane, demonstrating the scalability of this non-contact, large-area approach.

4.2 Single-atom catalysts

Single-atom catalysts (SACs), in which metal atoms are atomically dispersed on support materials, exhibit exceptionally high catalytic efficiency compared with bulk or nanoparticle-based catalysts because, in principle, nearly all metal atoms can participate in catalytic reactions without inactive regions [46-50]. Recently, the potential of SACs for gas-sensing applications has attracted significant attention. However, the precise synthesis of SACs with controlled metal type, loading density, and support material remains challenging, as conventional thermal treatment routes often induce atomic agglomeration driven by thermodynamic minimization of surface energy.

To overcome this limitation, Kim et al. introduced an FTS-based strategy to stabilize SACs on metal oxide supports [9]. As described above, simple mixing of a Pt precursor with SnO_2 supports followed by a single FTS pulse led to the formation of Pt nanoparticles (~2 nm) on SnO_2. Interestingly, when 10 consecutive pulses were applied to Pt precursor-coated SnO_2 nanosheets, single atoms or few-atom clusters were formed and stabilized on the SnO_2 surface, as confirmed by high-angle annular dark-field scanning transmission electron microscopy (HAADF-STEM) (Fig. 4(c)). Repeated flash-thermal shock likely fragmented the initially formed nanoparticles into progressively smaller clusters and ultimately isolated atoms. The mechanism could be further supported by density functional theory (DFT) calculations of the stabilization energies of Pt single atoms on Sn or O sites, and experimentally verified by X-ray absorption fine structure spectroscopy. This result highlights the potential of FTS to refine catalyst nanoparticles down to the atomic scale while stabilizing them on metal oxide supports. The ultrahigh temperatures generated during FTS likely provide sufficient activation energy for Pt dispersion, while the resulting metal–defect interactions promote thermodynamically favorable stabilization of isolated atoms.

In another study, Kim et al. demonstrated a one-step synthesis of SACs on N-doped graphene supports using a precursor mixture of graphene oxide, melamine as the nitrogen source, and metal salts as SAC precursors (Fig. 4(d)) [32]. After simple mixing, coating on a glass substrate, drying, and a single-pulse FTS treatment, the process induced sequential reduction of graphene oxide to reduced graphene oxide, decomposition of melamine with simultaneous nitrogen doping, and decomposition of the metal precursors, ultimately forming dense SACs anchored at N-coordinated sites. This approach enabled the formation of stable metal–N_4 moieties on N-doped reduced graphene oxide and demonstrated broad compositional versatility, encompassing Pt, Co, Ni, and Co–Ni dual single-atom systems, for both chemiresistive gas sensing and electrocatalytic applications.

4.3 Ex-solution catalysts

Ex-solution catalysts are catalytic nanoparticles that are partially socketed into the lattice of metal oxide scaffolds [51-53]. They are typically synthesized by first preparing metal-doped oxides and then annealing them at high temperature under a reducing atmosphere to induce ex-solution on the oxide surface. Because of their strong metal–support interaction, ex-solution catalysts exhibit excellent thermal stability and resistance to sulfur poisoning, which are particularly advantageous for metal oxide-based chemical sensors operating at elevated temperatures (200–450°C) [54-56].

In general, however, the ex-solution process requires several hours of high-temperature annealing in a reducing H_2 atmosphere, which is time- and energy-intensive and can degrade support materials, especially those that are not thermally stable or undergo severe phase transitions under reducing conditions. To address this limitation, Shin et al. reported an FTS-triggered ultrafast ex-solution process (Fig. 5(a)) [35]. In their approach, metal-doped WO_3 nanofibers were first prepared by electrospinning, followed by heat treatment, and a single FTS pulse subsequently induced the formation of dense Pt, Rh, and Ir ex-solved nanoparticles with sizes of ~5 nm on the WO_3 nanofiber scaffolds. Before FTS, no peaks corresponding to metallic nanoparticles were detected, and the WO_3 diffraction peaks instead reflected lattice distortion induced by Pt, Rh, and Ir dopants incorporated into the lattice within the solubility limit. After FTS, distinct Pt-, Rh-, and Ir-related XRD peaks appeared, and HRTEM further confirmed the formation of crystalline nanoparticles with clear lattice fringes. As expected, Pt ex-solved WO_3 nanofibers exhibited highly stable H_2S sensing performance during prolonged operation at high temperatures, and ex situ TEM analysis after long-term testing confirmed that the nanoparticles remained resistant to agglomeration.

In another study, Jang et al. showed that multielement ex-solution can also be achieved using FTS (Fig. 5(b)) [57]. They first synthesized Pt-, Pd-, and Ru-doped ZnO nanoparticles derived from ZIF-8, and subsequent FTS irradiation induced multielement ex-solution, producing PtPdRu alloy nanoparticles on the ZnO surface. DFT calculations revealed that the segregation energy was significantly reduced for PtPdRu ex-solution compared with single-element ex-solution, indicating a more favorable ex-solution process. Moreover, gas selectivity could be tuned by the composition of the ex-solved nanoparticles. For example, Pt-exsolved ZnO showed selectivity toward H_2S, whereas binary PtPd-exsolved ZnO

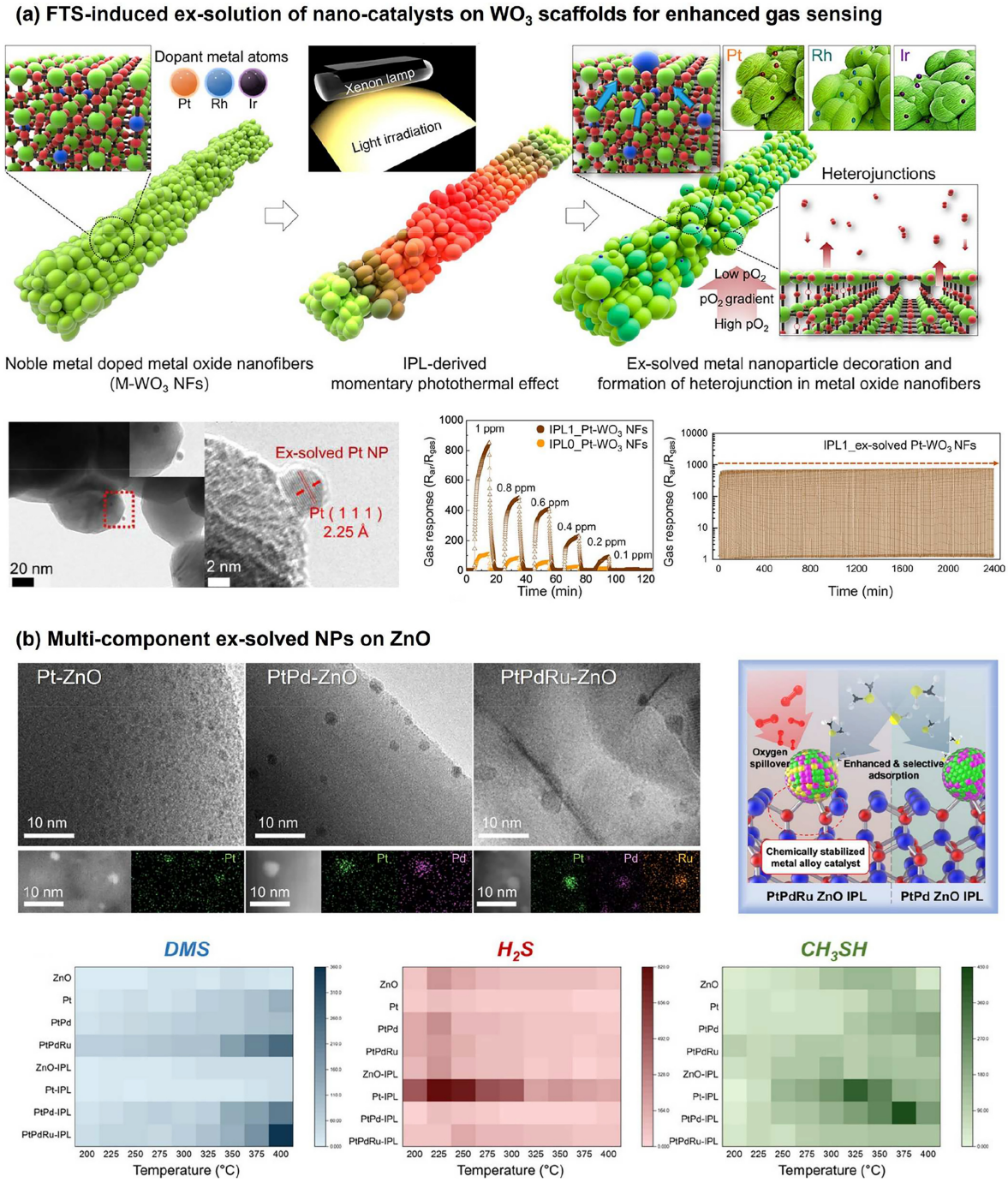

Fig. 5. Schematic illustrations of the FTS-induced ex-solution process from metal-doped metal oxides. (a) Ex-solution of single-component metal catalysts from WO_3 nanofibers and their high-performance H_2S sensing properties. Adapted from Ref. [35]. (b) Ex-solution of multicomponent nanoparticles from ZnO nanocubes and their tunable selectivity toward three sulfur-containing gas molecules. Adapted from Ref. [57].

and ternary PtPdRu-exsolved ZnO showed selectivity toward methyl mercaptan and dimethyl sulfide, respectively. Using this sensor array, successful gas identification and concentration prediction were achieved through machine-learning-based analysis.

Overall, FTS-derived catalyst strategies, including HEA catalysts, SACs, and ex-solution catalysts, can enhance chemical sensing performance by providing multielement or atomically dispersed active sites, promoting gas activation and interfacial charge transfer, and improving selectivity and operational stability through composition control and strong catalyst support interactions.

Table 2. Representative IPL-driven FTS processing conditions.

Material	Pulse number	Atmosphere	Temperature conditions	Photothermal material	Main outcome	Ref
Catalyst NPs@SnO_2	single pulse	Ambient-air	> 2073 K / 20 ms	Metal oxide nanosheet	Phase engineering / Ternary NPs	9
Single atom@ SnO_2	10 pulses	Ambient-air	> 2073 K / 20 ms	Metal oxide nanosheet	Single atoms	9
HEA@CNF	single pulse	Ambient-air	> 2073 K / 20 ms	Carbon nanofiber	High-entropy alloy	31
TMC@TMD core-shell	single pulse	Ambient-air	~ 3162 K / 10 ms	Graphene oxide	Core shell	33
Boron-doped rGO	single pulse	Ambient-air	~ 2073 K / 10 ms	Graphene oxide	Heteroatom doping	40
Ex-solved NPs@WO_3 nanofibers	single pulse	Ambient-air	> 1273 K / 20 ms	Metal oxide nanofiber	Ex-solved NPs	35
Single-atom@N-rGO	single pulse	Ambient-air	> 3123 K / 10 ms	Graphene oxide	Single atom	32

5. CONCLUSIONS AND PERSPECTIVES

IPL-driven FTS has emerged as a versatile platform for the design of kinetic materials beyond conventional rapid sintering. As summarized in Table 2, representative IPL-driven FTS studies demonstrate that diverse material transformations can be achieved in ambient air within millisecond-scale processing windows, typically within 20 ms. Its ultrafast heating and quenching characteristics enable nonequilibrium nanoengineering under ambient conditions, facilitating heteroatom doping, single-atom stabilization, high-entropy alloy synthesis, metastable phase formation, and controlled nanostructuring. These capabilities highlight FTS as a powerful route to advanced metastable functional materials.

Despite these advances, further process engineering is required to expand the versatility and controllability of FTS. Key challenges include accurate temperature measurement during millisecond-scale pulses, spatially resolved temperature-gradient analysis for large-area scalability and reproducibility, and precise control of the IPL processing atmosphere. In particular, atmosphere control is essential for overcoming limitations associated with the intrinsic oxygen affinity of constituent elements and for extending FTS beyond multielement hybridization toward diverse nonequilibrium compositions, including single-atom alloys, high-entropy oxides, carbides, sulfides, nitrides, and oxynitrides.

Hybrid process designs will also be important for practical implementation. Coupling FTS with external heating methods, such as Joule heating or induction heating, may enable more precise thermal control, while carbon-paper-based microfurnace strategies can expand FTS to materials with weak optical absorption (Fig. 6) [58]. In addition, solution-phase FTS using quartz cells could provide a promising route for uniform precursor delivery and scalable processing.

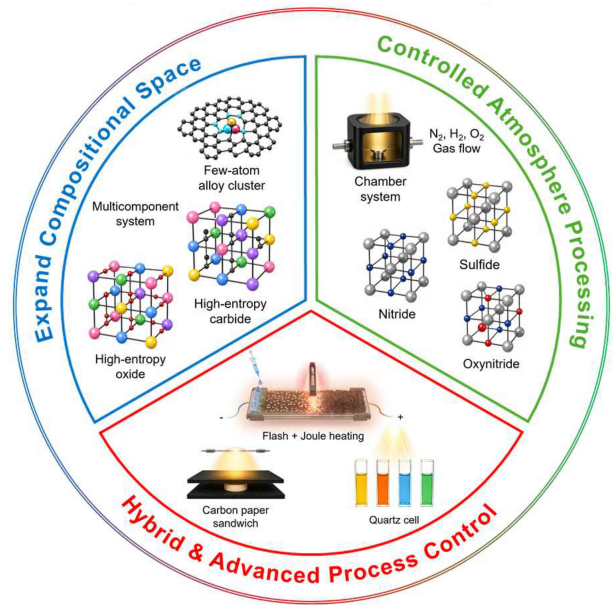

Fig. 6. Perspectives and future opportunities of FTS in the synthesis of advanced nanomaterials and catalysts.

Furthermore, the ultrashort thermal duration of FTS makes it a powerful platform for probing early-stage nucleation and phase-transition pathways. When combined with advanced characterization techniques such as atom probe tomography, 4D-STEM, and XAFS, FTS could reveal atomic-scale

photothermal processes, including atomic rearrangement, defect formation, compositional homogenization, and nonequilibrium phase stabilization. These studies will help establish FTS not only as a rapid synthesis method but also as a key platform for mechanistic understanding and rational nanomaterial design.

CRediT Authorship Contribution Statement

Suk-Jeong Kwon: Conceptualization, Investigation, Writing – original draft. **Sungwoo Eo:** Investigation, Writing – original draft. **Ji-Hwan Eum:** Investigation, Writing – review and editing. **Dong-Ha Kim:** Conceptualization, Funding acquisition, Investigation, Project administration, Writing – original draft, Writing – review and editing.

Declaration of Competing Interest

The authors declare that they have no known competing financial interests or personal relationships that could have influenced the work reported in this paper.

Acknowledgements

This work was supported by the Global Semiconductor Advanced Fab Utilization Project through the National NanoFab Center, funded by the Ministry of Science and ICT, Republic of Korea (No. RS-2025-14383333). This work was supported by the National Research Foundation of Korea (NRF) grant funded by the Korea government (MSIT) (No. RS-2024-00343700). This work was supported by Basic Science Research Program through the National Research Foundation of Korea (NRF) funded by the Ministry of Education (grant No. RS-2025-25396489).

REFERENCES

[1] P.M. Bulemo, D.-H. Kim, H. Shin, H.-J. Cho, W.-T. Koo, S.-J. Choi, et al., Selectivity in chemiresistive gas sensors: strategies and challenges, Chem. Rev. 125 (2025) 4111–4183.
[2] J.W. Baek, E. Shin, J. Lee, D.-H. Kim, S.-J. Choi, I.-D. Kim, Present and future of emerging catalysts in gas sensors for breath analysis, ACS Sens. 10 (2024) 33–53.
[3] H. Kim, J. Lee, Highly sensitive and selective gas sensors using p-type oxide semiconductors: overview, Sens. Actuators B 192 (2014) 607–627.
[4] J. Lee, Gas sensors using hierarchical and hollow oxide nanostructures: overview, Sens. Actuators B 140 (2009) 319–336.
[5] T.H. Im, J.H. Lee, H.S. Wang, S.H. Sung, Y.B. Kim, Y. Rho, et al., Flashlight-material interaction for wearable and flexible electronics, Mater. Today 51 (2021) 525–551.
[6] L. Eddy, S. Xu, C. Liu, P. Scotland, W. Chen, J.L. Beckham, et al., Electric field effects in flash joule heating synthesis, J. Am. Chem. Soc. 146 (2024) 16010–16019.
[7] R. Ye, D.K. James, J.M. Tour, Laser-induced graphene, Acc. Chem. Res. 51 (2018) 1609–1620.
[8] H. Lim, S. Kim, H. Jang, J. Lim, Intense pulsed light for split-second structural development of nanomaterials, J. Mater. Chem. C 5 (2017) 7142–7160.
[9] D.-H. Kim, J.-H. Cha, G. Shim, Y.H. Kim, J.-S. Jang, H. Shin, et al., Flash-thermochemical engineering of phase and surface activity on metal oxides, Chem 8 (2022) 1014–1033.
[10] S. Guo, M. Gao, W. Zhang, F. Liu, X. Guo, K. Zhou, Recent advances in laser-induced synthesis of MOF derivatives, Adv. Mater. 35 (2023) 2303065.
[11] S. Han, S. Hong, J. Yeo, D. Kim, B. Kang, M.-Y. Yang, S.H. Ko, Nanorecycling: monolithic integration of copper and copper oxide nanowire network electrode through selective reversible photothermochemical reduction, Adv. Mater. 27 (2015) 6397–6403.
[12] Z. Guo, Z. Liu, J. Zhang, J. Luo, X.-S. Tao, J. Ding, et al., Joule heating ultrafast synthesis, ACS Appl. Energy Mater. 8 (2025) 9926–9937.
[13] S. Dąbrowska, T. Chudoba, J. Wojnarowicz, W. Łojkowski, Current trends in the development of microwave reactors for the synthesis of nanomaterials in laboratories and industries: a review, Crystals 8 (2018) 379.
[14] A.M. Schwenke, S. Hoeppener, U.S. Schubert, Synthesis and modification of carbon nanomaterials utilizing microwave heating, Adv. Mater. 27 (2015) 4113–4141.
[15] Y. Su, Y. Zhang, Carbon nanomaterials synthesized by arc discharge hot plasma, Carbon 83 (2015) 90–99.
[16] Y. Chen, Y. Li, Y. Wang, K. Fu, V.A. Danner, J. Dai, et al., Rapid, in situ synthesis of high capacity battery anodes through high temperature radiation-based thermal shock, Nano Lett. 16 (2016) 5553–5558.
[17] C. Choi, J. Tour, Ultrafast and scalable materials synthesis with flash-within-flash Joule heating, Nat. Chem. 16 (2024) 1753–1754.
[18] Y. Liu, R. Lin, B. Guo, C. Chen, Q. Wu, X. Zhang, et al., Ultrafast Joule heating technology for functional nanomaterials synthesis: recent progress, challenges, and perspectives, Mater. Rep. Energy 5 (2025) 100377.
[19] H. Fujiwara, S. Daikokuya, T. Mirokuin, K. Hayashi, M. Matsuzaka, Y. Ohashi, et al., Site-specific synthesis of conductive graphitic nanomaterials on a NiFe thin film by localized laser irradiation, ACS Appl. Nano Mater. 6 (2023) 13885–13893.
[20] W. Devina, I. Subiyanto, D. Dung, S. Han, H. Yoon, D. Van Lam, et al., Rapid synthesis of nanomaterials by solvent-free laser irradiation for energy storage and conversion, Chem. Phys. Rev. 4 (2023) 041308.
[21] G. Xiong, J. Jia, L. Zhao, X. Liu, X. Zhang, H. Liu, et al., Non-thermal radiation heating synthesis of nanomaterials, Sci. Bull. 66 (2021) 386–406.
[22] I. Bilecka, M. Niederberger, Microwave chemistry for inorganic nanomaterials synthesis, Nanoscale 2 (2010) 1358–1374.
[23] V. Chikan, E.J. McLaurin, Rapid nanoparticle synthesis by magnetic and microwave heating, Nanomaterials 6 (2016) 85.

[24] N. Devi, S. Sahoo, R. Kumar, R. Singh, A review of the microwave-assisted synthesis of carbon nanomaterials, metal oxides/hydroxides and their composites for energy storage applications, Nanoscale 13 (2021) 11679–11711.
[25] A. Kiadehi, M. Jahanshahi, M. Mozdianfard, G. Vakili-Nezhaad, R. Seresht, Influence of the solution temperature on carbon nanotube formation by arc discharge method, J. Exp. Nanosci. 6 (2011) 432–440.
[26] Y. Liu, Z. Ge, Z. Li, Y. Chen, High-power instant-synthesis technology of carbon nanomaterials and nanocomposites, Nano Energy 80 (2021) 105500.
[27] J. Ng, Y. Raitses, Self-organisation processes in the carbon arc for nanosynthesis, J. Appl. Phys. 117 (2015) 063303.
[28] R. Dharmadasa, M. Jha, D. Amos, T. Druffel, Room temperature synthesis of a copper ink for the intense pulsed light sintering of conductive copper films, ACS Appl. Mater. Interfaces 5 (2013) 13227–13234.
[29] Y. Noh, G. Kim, H. Lee, J. Shin, K. An, M. Kumar, et al., A review on intense pulsed light process as post-treatment for metal oxide thin films and nanostructures for device application, Nanotechnology 33 (2022) 272001.
[30] Y. Noh, J. Shin, H. Lee, G. Kim, M. Kumar, D. Lee, Decoration of Ag nanoparticle on ZnO nanowire by intense pulsed light and enhanced UV photodetector, Chemosensors 9 (2021) 321.
[31] J.H. Cha, S.H. Cho, D.H. Kim, D. Jeon, S. Park, J.W. Jung, et al., Flash-thermal shock synthesis of high-entropy alloys toward high-performance water splitting, Adv. Mater. 35 (2023) 2305222.
[32] D.-H. Kim, J.-H. Cha, S. Chong, S.-H. Cho, H. Shin, J. Ahn, et al., Flash-thermal shock synthesis of single atoms in ambient air, ACS Nano 17 (2023) 23347–23358.
[33] E. Shin, D.H. Kim, M. Sagong, J. Choe, S.H. Park, J. Ahn, et al., Flash thermal shock synthesis of heterostructured transition metal dichalcogenides and carbides in milliseconds, Adv. Mater. 37 (2025) 2419790.
[34] L. Zhao, Y. Liu, R. Xing, X. Yan, Supramolecular photothermal effects: a promising mechanism for efficient thermal conversion, Angew. Chem. Int. Ed. 59 (2020) 3793–3801.
[35] E. Shin, D.-H. Kim, J.-H. Cha, S. Yun, H. Shin, J. Ahn, et al., Ultrafast ambient-air exsolution on metal oxide via momentary photothermal effect, ACS Nano 16 (2022) 18133–18142.
[36] D. Jeon, H. Shin, J. Cha, H. Kim, S. Park, J. Ahn, et al., Photothermal annealing-enabled millisecond synthesis of carbon nanoonions and simultaneous single-atom functionalization, ACS Nano 19 (2025) 34235–34247.
[37] A. Al-Hamry, H. Kang, E. Sowade, V. Dzhagan, R. Rodriguez, C. Müller, et al., Tuning the reduction and conductivity of solution-processed graphene oxide by intense pulsed light, Carbon 102 (2016) 236–244.
[38] S.-J. Choi, S.-J. Kim, I.-D. Kim, Ultrafast optical reduction of graphene oxide sheets on colorless polyimide film for wearable chemical sensors, NPG Asia Mater. 8 (2016) e315.
[39] S.J. Choi, S.J. Kim, J.S. Jang, J.H. Lee, I.D. Kim, Silver nanowire embedded colorless polyimide heater for wearable chemical sensors: improved reversible reaction kinetics of optically reduced graphene oxide, Small 12 (2016) 5826–5835.
[40] J.H. Cha, D.H. Kim, C. Park, S.J. Choi, J.S. Jang, S.Y. Yang, et al., Low-thermal-budget doping of 2D materials in ambient air exemplified by synthesis of boron-doped reduced graphene oxide, Adv. Sci. 7 (2020) 1903318.
[41] J.-H. Eum, S.-J. Kwon, S. Eo, D.-H. Kim, Tunable chemiresistive gas selectivity of thin-layered conductive metal-organic framework/reduced graphene oxide composites, ACS Sens. 11 (2026) 3840–3850.
[42] S. Choi, J. Jang, H. Park, I. Kim, Optically sintered 2D RuO_2 nanosheets: temperature-controlled NO_2 reaction, Adv. Funct. Mater. 27 (2017) 1606026.
[43] Y. Xin, S. Li, Y. Qian, W. Zhu, H. Yuan, P. Jiang, et al., High-entropy alloys as a platform for catalysis: progress, challenges, and opportunities, ACS Catal. 10 (2020) 11280–11306.
[44] Y. Yao, Z. Huang, P. Xie, S.D. Lacey, R.J. Jacob, H. Xie, et al., Carbothermal shock synthesis of high-entropy-alloy nanoparticles, Science 359 (2018) 1489–1494.
[45] Y. Yao, Q. Dong, A. Brozena, J. Luo, J. Miao, M. Chi, et al., High-entropy nanoparticles: synthesis-structure-property relationships and data-driven discovery, Science 376 (2022) eabn3103.
[46] Y. Chen, S. Ji, C. Chen, Q. Peng, D. Wang, Y. Li, Single-atom catalysts: synthetic strategies and electrochemical applications, Joule 2 (2018) 1242–1264.
[47] L. Li, X. Chang, X. Lin, Z.-J. Zhao, J. Gong, Theoretical insights into single-atom catalysts, Chem. Soc. Rev. 49 (2020) 8156–8178.
[48] G. Lei, H. Pan, H. Mei, X. Liu, G. Lu, C. Lou, et al., Emerging single atom catalysts in gas sensors, Chem. Soc. Rev. 51 (2022) 7260–7280.
[49] T. Chu, C. Rong, L. Zhou, X. Mao, B. Zhang, F. Xuan, Progress and perspectives of single-atom catalysts for gas sensing, Adv. Mater. 35 (2023) 2206783.
[50] Y. Yao, Z. Huang, P. Xie, L. Wu, L. Ma, T. Li, et al., High temperature shockwave stabilized single atoms, Nat. Nanotechnol. 14 (2019) 851–857.
[51] J.H. Kim, J.K. Kim, J. Liu, A. Curcio, J.-S. Jang, I.-D. Kim, et al., Nanoparticle ex-solution for supported catalysts: materials design, mechanism and future perspectives, ACS Nano 15 (2020) 81–110.
[52] O. Kwon, S. Sengodan, K. Kim, G. Kim, H.Y. Jeong, J. Shin, et al., Exsolution trends and co-segregation aspects of self-grown catalyst nanoparticles in perovskites, Nat. Commun. 8 (2017) 15967.
[53] B. Rudolph, A.I. Tsiotsias, B. Ehrhardt, P. Dolcet, S. Gross, S. Haas, et al., Nanoparticle exsolution from nanoporous perovskites for highly active and stable catalysts, Adv. Sci. 10 (2023) 2205890.
[54] D.-H. Kim, J.K. Kim, D. Oh, S. Park, Y.B. Kim, J. Ko, et al., Ex-solution hybrids functionalized on oxide nanofibers for highly active and durable catalytic materials, ACS Nano 17 (2023) 5842–5851.
[55] S. Park, D. Oh, J. Ahn, J.K. Kim, D.H. Kim, S. Kim, et al., Promoting ex-solution from metal-organic-framework-

mediated oxide scaffolds for highly active and robust catalysts, Adv. Mater. 34 (2022) 2201109.
[56] J.S. Jang, J.K. Kim, K. Kim, W.G. Jung, C. Lim, S. Kim, et al., Dopant-driven positive reinforcement in ex-solution process: new strategy to develop highly capable and durable catalytic materials, Adv. Mater. 32 (2020) 2003983.
[57] G.S. Kim, H. Kum, J.W. An, H. Kwon, Y.J. Ryu, H.W. Jang, et al., Ultrafast photothermal-shock-driven multimetallic exsolution for artificial olfaction of sulfur compounds detection, Small Struct. 6 (2025) 2500292.
[58] D. Jeon, H. Shin, J.-H. Cha, H. Kim, S. Park, J. Ahn, et al., Photothermal annealing-enabled millisecond synthesis of carbon nanoonions and simultaneous single-atom functionalization, ACS Nano 19 (2025) 34235–34247.

Suk-Jeong Kwon is an integrated M.S./Ph.D. student in the Department of Materials Science and Chemical Engineering at Hanyang University ERICA, under the supervision of Prof. Dong-Ha Kim. He received his B.S. degree in Materials Science and Engineering from Hanbat National University in 2025. His research focuses on nanomaterial-based chemiresistive gas sensors, electrocatalysts, and FAB-process-based ultra-low-power MEMS gas sensors, with an emphasis on controlling surface and interfacial properties for sensitive and selective chemical sensing.

Dong-Ha Kim is an Assistant Professor in the Department of Materials Science and Chemical Engineering at Hanyang University ERICA. He received his B.S. degree in Materials Science and Engineering from Hanyang University in 2016. He then earned his M.S. degree and Ph.D. degree in Materials Science and Engineering (2022), both from the Korea Advanced Institute of Science and Technology (KAIST). Following his doctoral studies, he conducted postdoctoral research in the Department of Chemistry at the Massachusetts Institute of Technology (MIT) from 2022 to 2024. His research focuses on tuning the surface activity of nanomaterials to achieve sensitive and selective detection of chemical species, with an emphasis on gaining fundamental insights into sensing mechanisms.